UDK 544.623:52-74
Original scientific article/Izvirni znanstveni članek

ISSN 1580-2949
MTAEC9, 56(1)19(2022)

POTENTIAL EFFECT OF UV RADIATION ON THE OPTICAL AND ANTI-MICROBIAL PROPERTIES OF PVA/METAL-SALT NANOCOMPOSITES

POTENCIALNI VPLIV ULTRA VIJOLIČNEGA SEVANJA NA OPTIČNE IN ANTI-MIKROBNE LASTNOSTI NANOKOMPOZITOV NA OSNOVI PVA IN KOVINSKIH SOLI

Huda Alkhaldi*, Zinab Alshorafa, Waheedh Albarqi, Manal Alzahrani, Mohamed Madani

Physics Department, College of Science and Humanitie-Jubail, Imam Abdulrahman Bin Faisal University, P.O.Box 12020, Jubail, Kingdom of Saudi Arabia

Prejem rokopisa – received: 2021-10-15; sprejem za objavo – accepted for publication: 2021-11-26

doi:10.17222/mit.2021.293

Polymer/metals nanocomposite films were investigated from aqueous solutions of polyvinyl alcohol (PVA)/acrylic acid (AAc) using UV radiation. The formation of metal nanoparticles (NPs) was characterized by transmission electron microscopy (TEM), Fourier-transform infrared spectrometry (FTIR) and UV-vis spectroscopy. It was found that UV radiation induced the reduction of the metal ions in the polymer matrix into metal nanoparticles. The electrical properties and the anti-microbial efficiency were carried out for the prepared compositions. The maximum AC conductivity was observed in the composites containing Ag NPs. Finally, a green method has been suggested for the development of conductive nano polymer/metal composites that can be used in biomedical applications.

Keywords: polyvinyl alcohol, UV-irradiation, optical, dielectric relaxation, anti-microbial

Avtorji v tem članku opisujejo raziskave sinteze nanokompozitnih filmov (tankih plasti) na osnovi polimerov in kovin izdelanih iz vodne raztopine polivinil alkohola (PVA) in akrilne kisline (AAc) z uporabo ultravijoličnega (UV) sevanja. Nastale kovinske nano delce (NPs) so okarakterizirali s presevnim elektronskim mikroskopom (TEM), furierjevo transformacijsko infrardečo spektroskopijo (FTIR) in UV-vis spektroskopijo. Avtorji ugotavljajo, da UV sevanje inducira redukcijo kovinskih ionov iz polimerne matrice v kovinske nano delce. Za pripravo različnih sestav so ugotavljali njihove električne lastnosti in njihovo anti-mikrobno učinkovitost. Maksimalno prevodnost izmeničnega toka (AC) so ugotovili pri sestavi, ki je vsebovala nanodelce na osnovi srebra (Ag). Na koncu prispevka še predlagajo novo metodo za razvoj prevodnih nano-kompozitov na osnovi kovinskih nano delcev s polimerno matrico za bio-medicinske aplikacije.

Ključne besede: polivinl alkohol, ultra vijolično sevanje, optika, dielektrična relaksacija, anti-mikrobnost

1 INTRODUCTION

Nanocomposite materials are formatted from two or more different chemical and physical phases that are separated by a discrete interface in a nanometre size.[1] Nano-materials have an enormous range of chemical and physical properties that rely on their shape and size.[2] Metal nanoparticles (NPs) combined with polymers are attracting considerable interest in both the research and industrial sectors due to their electrical, thermal, and optical properties. The properties of the final products depend on the physicochemical properties of the additives and the way that they link within the matrix.

PVA is a semi-crystalline polar polymer that is applied in this work as a host matrix owing to its properties and has numerous industrial technologies due to the presence of the characteristic hydrogen bonds and OH functional group formatted in its matrix.[3,4] The anti-microbial efficiency of metal NPs embedded PVA have been addressed and it was found that some of these metals have a significant antibacterial activity and can be used in biomedical applications.[5] The stability, morphology, filler distribution, and properties of PVA/metal NPs are strongly dependent on the incorporation method and processing conditions.[6] Recently, many researches were focused on the green and effective methods (irradiation) that can induce modification in the physicochemical properties of the polymeric materials such as polymer-chain scission, the rearrangement of bonding and the formation of carbon-rich clusters and the formation of new bonds.[7,8] The cross-linking of the polymer can be achieved by using an effective method such as the photo-curing technique, owing to the formation of functional groups that result from light-induced interactions.[9] UV-radiation processing technology is a useful tool for improving the polymer characteristics as well as its ability to induce a reduction for the formatted nanoparticles inside the matrix.[10] Radiation-induced grafting is a green tool for the preparation of low-cost and easily obtainable copolymers. Acrylic acid (AAc) grafted PVA prepared

*Corresponding author's e-mail:
hsalkaldi@iau.edu.sa (Huda Alkhaldi)

by radiation-induced grafting involve membranes and particular adsorbents for use in numerous applications.[11–13] Free radicals were formed during the irradiation on both the AAc and the polymers. Then a subsequent interaction between these free radicals leads to the formation of a network between the polymer backbone and the intermediates (and/or moieties) of AAc.

In this work, compositions of PVA/AAc embedded with different metal salts such as aluminium nitrate, silver nitrate and copper nitrate were investigated using UV-irradiation and measurements of the physical properties of the investigated samples were performed.

2 EXERIMENTAL PART

2.1 Materials

PVA powders was supplied by the Sigma-Aldrich company with an average molar mass of 130,000 g/mol, 99 % hydrolysed. Three different types of metal-salt additives were used, i.e., aluminium nitrate ($Al(NO_3)_3{\cdot}9H_2O$) provided from Techno Pharmchem Co, silver nitrate $AgNO_3$ provided from Rankem-India, copper nitrate ($Cu(NO_3)_2{\cdot}3H_2O$), anhydrous acrylic acid (AAc with (density 1.051 g/mL at 25 °C, molar mass 72.06 g/mol and purity 99 %) and photoinitiator of 2-hydroxy-4-(2-hydroxyethoxy)-2-methylpropiophenone ($C_{12}H_{16}O_4$) were supplied from Sigma-Aldrich, Germany.

2.2 Sample Preparation

Some 10 g of PVA were dissolved in 200 mL of distilled water and maintained in a water bath at 70 °C until it becomes viscous and transparent. Then acrylic acid solution was added to the PVA (40 *w*/% solution). A 3 *w*/% solution of PVA of $C_{12}H_{16}O_4$ was dissolved in ethanol and added to the solution to induced an effective photo-chemist solution. The metals salts were dissolved in distilled water and then added, separately, to the prepared solution with a fixed concentration of 10 *w*/% of PVA and then exposed to UV radiation for 20 min and then left to dry at room temperature. UV irradiation was carried out using a UV flooding curing lamp (Dymax ECE 2000 System). The intensity of the lamp was 400 W and the wavelength range (320–390 nm). PVA is a colourless polymer. The solutions of Ag-PVA, Cu-PVA and Al-PVA were turned brown, blue and white, respectively, during UV exposure, indicating the formation of metal ions in the polymer matrix. A schematic diagram showing the Ag^+ ion formation and UV-induced reduction of Ag NPs in Ag/PVA nanocomposite film is presented in **Figure 1**.

2.3 Characterization

FT-IR spectra were collected using a Fourier-transform infrared spectrometer (FTIR) (IRAfinity-Shimadzue) in the wavenumber range from 400 cm^{-1} to 4000 cm^{-1}.

The optical absorbances of the composites were measured in different ranges from 200 nm to 900 nm using a Shimadzu-UV2600 spectrophotometer.

A TEM-1011, with an operating voltage of 80 kV, was used to monitor the dispersion and size of the NPs within the polymer matrix. The magnification ranged from 50× to 600000×.

The dielectric measurements of the investigated composites were executed at ambient temperature using a HIOKI- Hitester LCR (Japan) in the frequency range from 100 Hz to 5 MHz.

2.4 Disc diffusion test (anti-microbial activity)

Agar plate diffusion test is commonly used to examine the possibility of using such films as anti-bacterial agents. Strips of 8 mm in diameter containing different types of metal NPs were place in agar with bacteria, and the plate left for 24 h. A free zone around the sample was

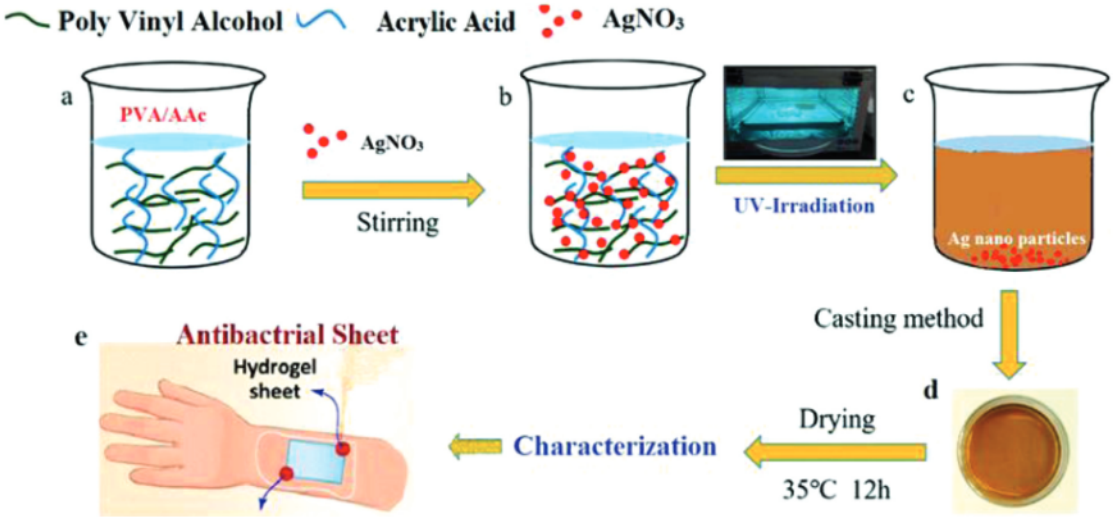

Figure 1: Formation of Ag nanoparticles inside biofilms against human pathogens using the UV-irradiation technique

formed, if the tested sample stops the bacteria from growing. The microorganisms chosen in this work to test the antibacterial properties were Escherichia coli, Gram-ve, and Staphylococcus aureus, Gram +ve.

3 RESULTS AND DISCUSSION

3.1 Characterizations of samples

To confirm the formation of metal nanoparticles inside the polymer matrix, images of Ag/PVA-g-AAc, Al/PVA -g-AAc and Cu/PVA-g-AAc were collected from TEM, as can be seen in **Figure 2**.

It is clear from the image that the formation of spherical metal NPs (shown as black spots) and the NPs are well dispersed in a polymer matrix without any large aggregation from the metal particles. It was reported that the particle size of the NPs is greatly affected by the type of metals.[8] The average size of Ag, Al and Cu is about (25; 10; 25) nm, respectively.

The small size of the formed NPs may be due to the restricted space of the PVA-g-AAc macromolecular chains, which limit the growth of the NPs during the irradiation process.[11]

3.2 FTIR analysis

Vinyl alcohol and vinyl acetate groups are the main chain in the PVA. Previous studies showed that adding AAc into PVA will produce a new intermolecular bond between the hydroxyl -OH group of the PVA and carboxylic acid group of the AAc.[11] A FTIR analysis conducted to verify the significant changes in the functional groups of PVA-g-AAc compared with the irradiated PVA, as can be seen in **Figure 4**. **Figure 4a** shows the absorption bands for the irradiated cross-linked PVA. No significant alteration in the characteristic absorption

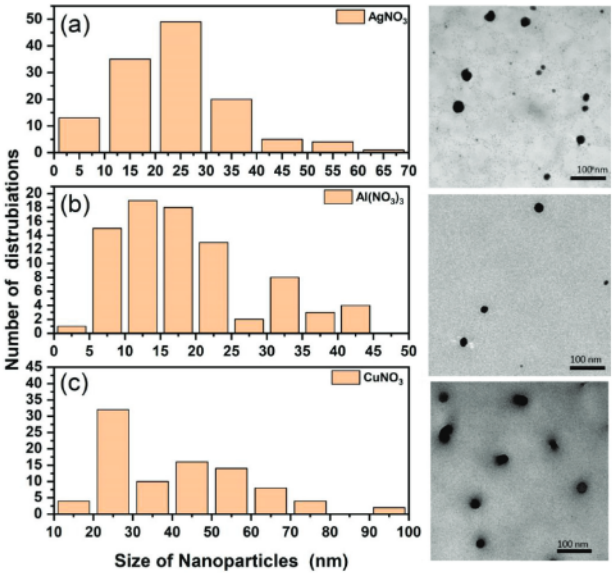

Figure 2: TEM images of: a) Ag NO_3/PVA-g-AAc, b) Al $(NO_3)_3$/PVA-g-AAc, c) Cu NO_3/PVA-g-AAc

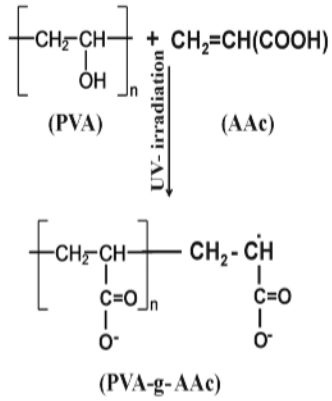

Figure 3: Free-radical polymerization and intermolecular bond formation of the acrylic acid monomer into PVA matrix

bands of PVA was observed based on the previous studies.[12] The characteristic peaks at 2975 cm^{-1}, 1661 cm^{-1} and 1107 cm^{-1} are related to the vibrations of the C-H group, C=O acetyl group and C-O group, respectively, of PVA. A band at 2975 cm^{-1} and another close one starts from 2816–2881 cm^{-1} are due to the presence of CH_2 stretching vibrations.[13] However, by grafting with AAc, **Figure 4b**, the band intensity of the O–H stretching becomes weaker and slightly shifted towards a low wavenumber of 3608 cm^{-1} compared to the crosslinked PVA. A new characteristic peak was detected at 1736 cm^{-1} associated with C=O group of AAc. Significantly, the broad band starting from 1641–1736 cm^{-1} was indicated as the formation of carboxylic/ester group in the network. The suggested link for the intermolecular bond formation copolymerization between acrylic acid and PVA is presented in **Figure 3**.

FTIR spectra of the PVA-g-AAc doped, separately, with 10 *w*/% of $Cu(NO_3)_2$, $Al(NO_3)_3$, and $AgNO_3$, are presented in **Figure 4c**, respectively. It was reported that the hydroxyl group can interact with the inorganic metal.[13] The change and shift in the peak intensity of

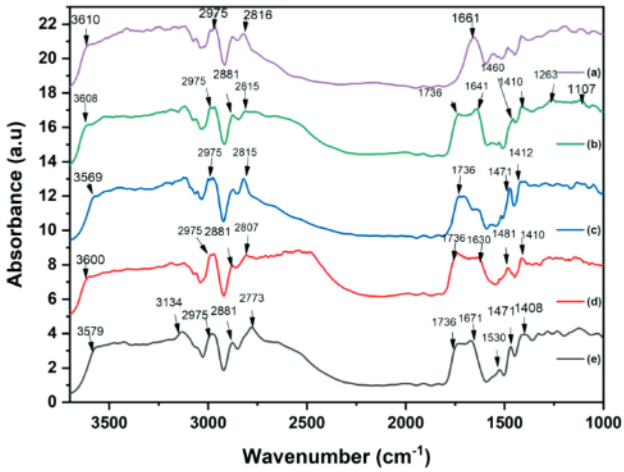

Figure 4: FTIR spectra: a) cross-linked PVA, b) PVA-g-AAc, c) Cu NO_3/PVA-g-AAc, d) Al $(NO_3)_3$/PVA-g-AAc, e) Ag NO_3/PVA-g-AAc

PVA-g-AAc are due to the creation of a charge-transfer complex between the ion metals and the polymer matrix.[14] The absorption wavenumber of the hydroxyl group of the PVA-g-AAc shifted from 3608 cm^{-1} to 3569 cm^{-1}, 3600 cm^{-1} and 3579 cm^{-1} in Cu/PVA-g-AAc, Al/PVA-g-AAc and Ag/PVA-g-AAc, respectively. This gives an indication of the interaction between PVA and the inorganic metals. Moreover, the intensity of the peak at 2975 cm^{-1} of the absorption band become weaker and shifted to lower frequency in all the metal-doped samples. This was assigned by the CH stretching vibration of the CH_2 between the PVA and the doped inorganic metals.

A band observed at 1736–1630 cm^{-1} associated with the acetyl group C=O due to the addition of the Cu metal. The intensity became weaker and shifted to a lower wavelength compared with PVA-g-AAc. This indicated the decreasing quantity in the Chelating group, which is becoming more obvious with the bonded with carboxylate group in AAc.[11] In addition, a broad band at 2406–2815 cm^{-1}, for Ag/PVA-g-AAc shifted to higher frequencies, while Al/PVA -g-AAc shifted to lower frequencies. For Cu/PVA-g-AAc the band disappeared, which indicates that chelating of each metal with the hydroxyl group in PVA chains.

3.3 UV-vis spectroscopy

UV-vis spectral analysis was employed for PVA-g-AAc embedded, separately, with 10 *w*/% of $AgNO_3$, $Al(NO_3)_3$ and $Cu(NO_3)_2$ in the range 200–900 nm. The optical band gaps (E_g) were analysed using these spectra. **Figure 5** presents the UV-vis spectra with a discrete absorption band for Ag/PVA-g-AAc at 435 nm. It is obvious that this peak is due to the formation of Ag metal NPs linked with the polymer matrix. These peaks were because of a π–π^* transition from unsaturated bonds which are C=O, and/or C=C in the polymer.[15]

The absorption coefficient (α) was estimated using the attenuation relation $I = I_0 \exp(-\alpha \cdot X)$ using the Mott and Davis model:[16]

$$\alpha(\lambda) = 2.303AX^{-1} \quad (1)$$

where X represents the film thickness, λ is the wavelength of the UV light and A is the absorbance calculated from $A = \log(I_0/I)$. I and I_0 represent the intensities of the transmitted and incident light, respectively. Based on the fundamental absorption, the band gap (E_g) separated between the conduction band (CB) and valence band (VB) of the samples was determined. This correlated with the electron transferred from VB to the CB.[17] In order to calculate the E_g of the various metal-doped PVA-g-AAc, the following Equation (2) was used:

$$(\alpha h\nu)^{1/n} = \alpha_0(h\nu - E_g) \quad (2)$$

where α_0 considered as an energy-independent constant, $h\nu$ is the energy of incident photons and n is constant,

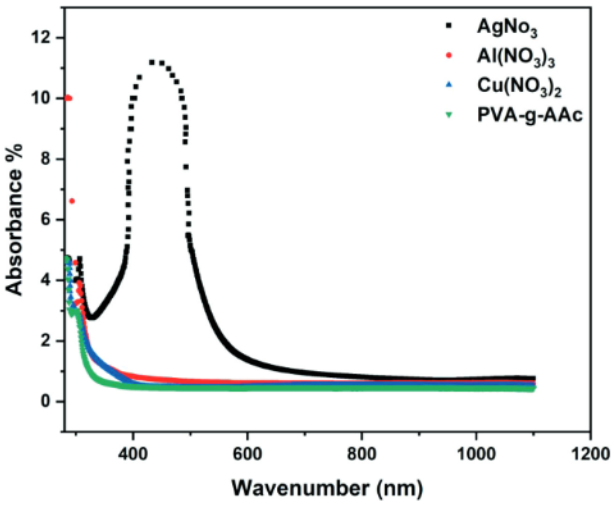

Figure 5: Absorbance versus wavelength for PVA-g-AAc doped with different metals

which demonstrates the optical transition method in the k-space.

The relation between $(\alpha\ h\nu)^{1/n}$ and incident light energy ($h\nu$) gives curve fit either on the direct transition n (1/2; 3/2), or indirect transition where the n (2; 3).[18–20] **Figure 6** shows that the best fit was at $n = 2$. This gives an indication of the indirect transition of the electrons in k-space.[7] The values of E_g were calculated by extrapolating of the linear portion of $(\alpha\ h\nu)^{1/2}$ and ($h\nu$) to zero absorption on the horizontal axis. The determined values of E_g are presented in **Table 1**. The E_g of the non-embedded irradiated PVA-g-AAc was 4.8 eV, which reduced to (3.06; 3.55; 3.3) eV for samples embedding with $AgNO_3$, $Al(NO_3)_3$, and $Cu(NO_3)_2$, respectively. These noticeable decreases in the band energy open the door to the possibility of using such composites in some optical applications.

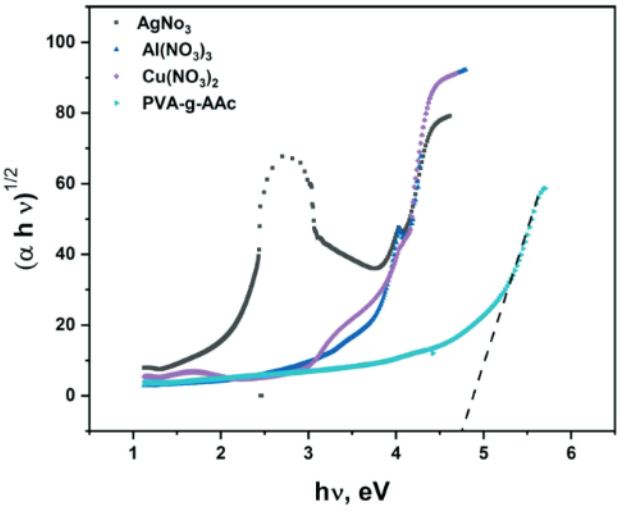

Figure 6: Plots of $(\alpha \cdot h\nu)^{1/2}$ vs. energy for various films

3.3 Dielectric analysis

The dielectric permittivity (ε') expresses the amount of energy stored in a system during a periodic electrical excitation. This stored energy is ordinarily in the form of an irregular distribution of dipoles or layers from ionic charge.[21] The dielectric constant can be evaluated using Equation (3):

$$\varepsilon' = \frac{C}{C_0} \quad \text{and} \quad C_0 = \varepsilon_0 \frac{A}{d} \tag{3}$$

where C is the measured capacitance of the sample and d is its thickness, C_0 is the vacuum capacitance, A is the electrode area and the vacuum permittivity $\varepsilon_0 = 8.85 \times 10^{-12}$ F/m.

The dielectric loss factor (ε") that describes the energy loss factor of a matrix due to periodic electric excitation was obtained from (tan δ being measured using Equation (4):

$$\tan\delta = \frac{\varepsilon''}{\varepsilon'} \tag{4}$$

The presence of moving dipoles or viscous drag leads to energy loss, which typically corresponds to the electrical conductivity of the substance.

Figures 7a and **7b** represents the frequency dependence of ε' and ε", respectively, at room temperature for PVA-g-AAc and PVA-g-AAc imbedded with different metal salts, separately. Both ε' and ε" decrease with an increased frequency in the low-frequency region. This is possibly due to the polarization effects of the electrode–electrolyte interface.[22] ε' and ε", which are used to describe the molecular relaxations, are influenced by different factors such as dielectric relaxation of polarized dipoles in the matrix, interfacial layers (interfacial polarization), and interface/surface states and their relaxation time (Maxwell–Wagner–Sillars relaxation). Both the interfacial polarization and the dipole orientation take place at low and intermediate frequencies.

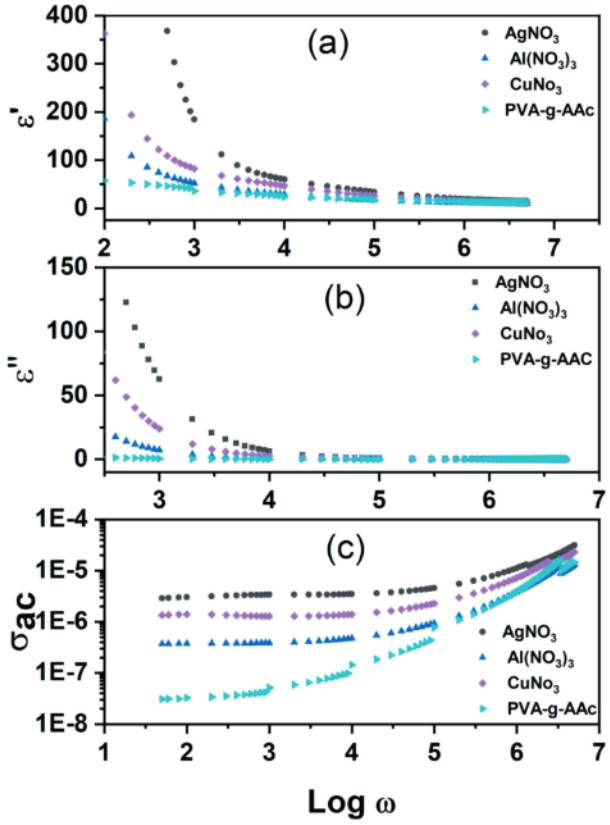

Figure 7: Frequency dependence: a) dielectric constant, b) dielectric loss, c) AC conductivity for the prepared samples

At low frequencies of less than 1 MHz, surface states or traps be able to pair the cyclic exchange of the electric field mutually and produce an excess of charge.[23] The dipole polarization and interpolarization were explained by the Maxwell-Wagner relaxation.

At higher frequencies above 1 MHz, the interface traps cannot contribute to an overcharge because the charges in these traps cannot follow the cyclic exchange of the electric field. The cyclic exchange of the electric field happens so rapidly at high frequencies that dipoles are not able to align in the field's direction at high frequencies. The polarization effect due to the charge accumulation decreased, resulting in a decrease in the value of ε' and ε".[24]

It was observed that the samples containing metals NPS have a higher ε' and ε" values compared to non-embedded PVA-g-AAc. The composites containing Ag NPs have a higher ε' followed by that containing Cu and then those containing Al.[25] The dielectric nature of the films containing minerals is higher due to the formation of many free ions in the matrix, therefore, the capacitance of the two-layer electrolytic capacitors has a higher value, and consequently the conductivity of the composites becomes better.

3.4 AC conductivity

The AC conductivities of the PVA-g-AAc/metals composites were analysed to introduce a much better understanding of the conduction method. The AC conductivity $\sigma_{AC}(\omega)$ was calculated using Equation (5):

$$\sigma_{AC}(\omega) = \omega\varepsilon_0\varepsilon'', \quad \omega = 2\pi f \tag{5}$$

The conductivity dependence on frequency of the PVA-g-AAc/metals polymer electrolytes at room temperature is shown in **Figure 7c**. The existence of moving dipoles leads to energy loss, which usually goes along with the electrical conductivity of the substance. With increasing frequency, the conductivity values of the studied composites increased. Low-frequency dispersion is caused by interfacial resistance or the accumulation of space charges.[25] In the low-frequency region, as the frequency increases, the polarization occurred at the electrode and electrolyte interface decrease, which induced a decrease in the eddy currents, and eventually decreases the loss tan δ.[26] In the high-frequency region, the ion mobility increases with frequency and consequently higher

values of conductivity were detected. Composites containing metal NPs have a higher σ_{AC} values compared to non-embedded PVA-g-AAc. The sample containing silver has the highest conductivity values, followed by copper and finally Al. These results agree with the calculated E_g values which represented in **Table 1**.

Table 1: Optical band gap, relaxation time and anti-microbial activity of all compositions

Sample	E_g/(eV)	τ/μs	inhibition zone diameter (mm)	
			Gram -ve *Escherichia coli*	Gram +ve *Staphylococcus aureus*
PVA-g-AAc	4.8	–	0 ± 0	0 ± 0
$AgNO_3$	3.06	53	11 ± 1	6 ± 6
$Cu(NO_3)_2$	3.3	265	6 ± 6	6 ± 3
Al $(NO_3)_3$	3.55	397	–	–

3.5 Modulus formalism

The analysis of the electrical properties of dielectric materials is used to extract the complex electrical modulus (M^*), through which certain phenomena such as electrode polarization and conductivity relaxation times can be discussed. The electric modulus formalism M^* is calculated by transforming the dielectric data $\varepsilon^*(\omega) = \varepsilon'(\omega) - i\varepsilon''(\omega)$ (Equation (6)):[22]

$$M^*(\omega) = \frac{1}{\varepsilon'^*(\omega)} = M'(\omega) + iM''(\omega) \quad (6)$$

where M' and M'' are the real and imaginary components of the electric modulus M^*. In the low-frequency range, the zero values of M' denote the polarization effects of the electrode-electrolyte interface.[6] While the ionic segmental motions in the polymers can be determined from the main characteristic peak of M'' situated at a certain frequency.[25,26]

The values of M' and M'' were evaluated using the following Equation (7):

$$M'(\omega) = \frac{\varepsilon'(\omega)}{\varepsilon'^2(\omega) + \varepsilon''^2(\omega)}, \quad M''(\omega) = \frac{\varepsilon''(\omega)}{\varepsilon'^2(\omega) + \varepsilon''^2(\omega)} \quad (7)$$

The frequency dependence of the real and imaginary components (M' and M'') of the modulus for the investigated samples are presented in **Figures 8a** and **8b**, respectively. As shown in **Figure 8a** the value of M' increases exponentially with the frequency. It approaches zero at very low frequencies, and increases slightly, indicating the effect of electrode polarization.[27] The gradual increase of the M' values with increasing frequency (at f = 0.5 MHz) are due to the dielectric relaxation of the polarized charges. At frequencies more than 0.5 MHz, the value of M' increases dramatically until it reaches a maximum value for all the samples due to the relaxation process which corresponds $M_8 = 1/\varepsilon_8$.[27]

The spectrum analysis of M'' shows a well-defined asymmetrical peak, which confirms the existence of the relaxation times (τ). The relaxation time can be calculated from $\omega_{max}\ \tau = 1$, where ω_{max} is the relaxation frequency at the peak maximum, which is assigned to the dipole relaxation. The relaxation times τ were calculated and tabulated in **Table 1** for the complexes embedded with the metal NPs. The relaxation time is inversely proportional to the σ_{AC} values of the composites, which confirms that the conduction along the coordinate sites of the matrix depends on the relaxation time of the ionic charges.[28]

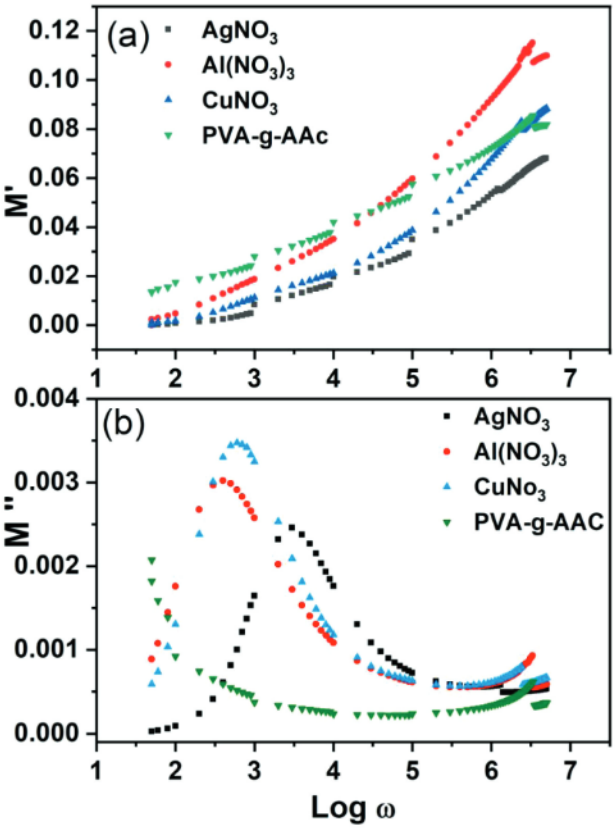

Figure 8: Modulus of prepared composites: a) real part of modulus (M'), b) imaginary part of modulus (M'') versus frequency

The dependence of the dielectric properties on the frequency show two relaxation processes. First, at lower frequencies, the relaxation process is due to the Maxwell-Wagner relaxation. While the second relaxation process, which appeared at medium frequencies, it is the result of ionic conduction relaxation. Studies of the AC conduction and modulus of the composites alternating support the hopping mechanism of conduction in these compositions. It can be concluded that the conduction in the matrix depends mainly on type of metal ions and the microstructure within the polymer matrix.

3.6 Anti-microbial analysis

To investigate the antibacterial activity of the copper, silver, and aluminium NPs, two microorganisms were used, namely, E. coli and S. aureus bacteria. The determination of the bacteria's activity utilized the diameter of the inhibition zone by disc diffusion test. The sensitiv-

ity of the microorganisms can be evaluated by measuring the diameter of the inhibition zone. **Table 1** shows the antibacterial study results. A larger diameter zone was recorded in Ag NPs around 11 mm for E. Coli, and 6 mm for S. aureus. While Cu NPs gives the maximum inhibition zone with a 6 mm diameter against E. coli and 6 mm diameter for S. aureus. The Al NPs do not exhibit any active result. Bactericide is sensitive to certain types of metals (noble metals) and depends mainly on the type and the size of the metal surface.[29]

4 CONCLUSIONS

We have reported on the UV-irradiation-induced grafting of PVA/acrylic acid copolymer and embedded with different inorganic nitrate salts using the casting method. The successfully fabricated metal NPs were an average particle size of (25; 10; 25) nm for Ag, Al and Cu respectively. These results were confirmed by TEM analyses. The optical analysis exhibited indirect optical energy gap E_g have the values of (4.8; 3.06; 3.3; 3.55) eV for PVA-g-AAc, Ag, Cu and Al embedded in the matrix. The compositions doped with Ag salts have the highest electrical conductivity and produce smaller nano-scaled particles, followed by copper and finally aluminium salts. FTIR studies helped us to understand the change in intensity, the position of the peaks, which also confirm the complexation of PVA/AAc and metal-salts systems. The anti-microbial activity test indicated that Ag and Cu have the highest dimeter inhibition zone and are recommended for use in biomedical applications.

5 REFERENCES

[1] S. B. Aziz, H. M. Ahmed, A. M. Hussein, A. B. Fathulla, R. M. Wsw, R. T. Hussein, Tuning the absorption of ultraviolet spectra and optical parameters of aluminum doped PVA based solid polymer composites, J. Mater. Sci. Mater. Electron., 26 (**2015**) 10, 8022–8028, doi:10.1007/s10854-015-3457-6

[2] A. Abbas, R. Naife, F. Lafta, A. Hashim, Optical Properties of (PVA-PAA-Ag) Nanocomposites, Int. J. Sci. Res., 4 (**2015**) 1, 2489–2491

[3] A. Tawansi, A. El-Khodary, M. M. Abdelnaby, A study of the physical properties of FeCl3 filled PVA, Current Applied Physics, 5 (**2005**) 6, 572–578, doi:10.1016/j.cap.2004.06.026

[4] M. K. El-Mansy, E. M. Sheha, K. R. Patel, G. D. Sharma, Characterization of PVA/CuI polymer composites as electron donor for photovoltaic application, Optik (Stuttg)., 124 (**2013**) 13, 1624–1631, doi:10.1016/j.ijleo.2012.05.009

[5] S. Horiike, S. Matsuzawa, K. Yamaura, Preparation of chemically crosslinked gels with maleate-denatured poly(vinyl alcohol) and its application to drug release, J. Appl. Polym. Sci., 84 (**2002**) 6, 1178–1184, doi:10.1002/app.10411

[6] D. M. Alshangiti, M. Madani, Nano-Ag Doping Induced Changes in the Optical Behavior and Thermal Stability of Acrylic Acid-Grafted Poly Vinyl Alcohol Copolymer Films, Polym. Plast. Technol. Eng., 53 (**2014**) 13, 1385–1391, doi:10.1080/03602559.2014.909471

[7] A. M. Ismail, M. I. Mohammed, E. G. El-Metwally, Influence of Gamma irradiation on the structural and optical characteristics of Li ion-doped PVA/PVP solid polymer electrolytes, Indian J. Phys., 93 (**2019**) 2, doi:10.1007/s12648-018-1286-1

[8] J.-P. Fouassier, J. F. Rabek, Radiation curing in polymer science and technology: Practical aspects and applications, Vol. 4. Springer Science Ð& Business Media, (1993)

[9] M. A. Khan, S. K. Bhattacharia, M. A. Kader, K. Bahari, Preparation and characterization of ultra violet (UV) radiation cured bio-degradable films of sago starch/PVA blend, Carbohydr. Polym., 63 (**2005**) 4, 500–506, doi:10.1016/j.carbpol.2005.10.019.

[10] M. Eid, D. Hegazy, Electron Beam Synthesis and Characterization of Poly Vinyl Alcohol/Poly Acrylic Acid Embedded Ni and Ag Nanoparticles, J. Inorg. Organomet. Polym. Mater., 22 (**2012**) 5, doi:10.1007/s10904-012-9683-y

[11] Y. Luo, X. Jiang, W. Zhang, X. Li, Effect of Aluminium Nitrate Hydrate on the Crystalline, Thermal and Mechanical Properties of Poly(Vinyl Alcohol) Film, Polym. Polym. Compos., 23 (**2015**) 8, 555–562, doi:10.1177/096739111502300805

[12] R. S. Hafez, S. El-Khiyami, Effect of copper (II) nitrate $3H_2O$ on the crystalline, optical and electrical properties of poly(vinyl alcohol) films, J. Polym. Res., 27 (**2020**) 2, 26, doi:10.1007/s10965-019-1993-0

[13] R. P. Chahal, S. Mahendia, A. K. Tomar, S. Kumar, SHI irradiated PVA/Ag nanocomposites and possibility of UV blocking, Opt. Mater. (Amst)., 52 (**2016**), 237–241, doi:10.1016/j.optmat.2015.12.049

[14] T. Jayaramudu, Y. Li, H.-U. Ko, I. Shishir, J. Kim, Poly(acrylic acid)-Poly(vinyl alcohol) hydrogels for reconfigurable lens actuators, Int. J. Precis. Eng. Manuf. Technol., 3 (**2016**), 375–379, doi:10.1007/s40684-016-0047-x

[15] B. Singh, V. Sharma, Design of psyllium–PVA–acrylic acid based novel hydrogels for use in antibiotic drug delivery, Int. J. Pharm., 389 (**2010**) 1, 94–106, doi:10.1016/j.ijpharm.2010.01.022

[16] E. Mott, N. F. Davis, Electronic Processes in Non-Crystalline Materials. UK: Oxford University Press: Oxford, (1979)

[17] S. H. Shinde, V. R.; Gujar, T. P. Lokhande, C. D. Mane, R. S. Han, Mn doped and undoped ZnO films: A comparative structural, optical and electrical properties study, Mater. Chem. Phys., 389(2010) 1, 94–106, doi.org/10.1016/j.matchemphys.2005.07.045

[18] O. Monroy, L. Fomina, M. Sánchez-Vergara, G. A. Vázquez-Hernández, L. Alexandrova, R. Gaviño, L. Rumshd, M. G. Zolotukhin, R. Salcedo, Synthesis, characterization and evaluation of optical band gap of new semiconductor polymers with N-aryl- 2,5-diphenyl-pyrrole units, J. Mol. Struct., 1245 (**2021**), 131012, doi:10.1016/j.molstruc.2021.131012

[19] S. Pervaiz, N. Kanwal, S. A. Hussain, M. Saleem, I. A. Khan, Study of structural, optical and dielectric properties of ZnO/PVDF-based flexible sheets, J. Polym. Res., 28 (**2021**) 8, 309, doi:10.1007/s10965-021-02640-9

[20] S. S. Bulla, R. F. Bhajantri, C. Chavan, Optical and Structural Properties of Biosynthesized Silver Nanoparticle Encapsulated PVA (Ag–PVA) Films, J. Inorg. Organomet. Polym. Mater., 31 (**2021**) 6, 2368–2380, doi:10.1007/s10904-021-01909-2

[21] A. M. Motawie, M. Madani, E. A. Esmail, A. Z. Dacrorry, H. M. Othman, M. M. Badr, D. E. Abulyazied, Egypt. J. Pet. 23 (**2014**), 379–387, doi:10.1016/j.ejpe.2017.06.004

[22] M. Madani, S. S. Aly, S. M. El-Sayed, Dielectric Relaxation of New Aniline Methyl Methacrylate Copolymer Synthesized by Gamma Irradiation Initiated Polymerization, High Perform. Polym., 22 (**2010**) 5, 515–533, doi:10.1177/0954008309345551

[23] M. Madani, Effect of silica type and concentrations on the physical properties of EPDM cured by γ -irradiation, Mol. Phys., 106 (**2008**) 7, 849–857, doi:10.1080/00268970801980484

[24] S. Mahendia, A. K. Tomar, S. Kumar, Electrical conductivity and dielectric spectroscopic studies of PVA–Ag nanocomposite films, J. Alloys Compd., 508 (**2010**) 2, 406–411, doi:10.1016/j.jallcom.2010.08.075

[25] D. K. Pradhan, R. N. P. Choudhary, B. K. Samantaray, Studies of dielectric relaxation and AC conductivity behavior of plasticized polymer nanocomposite electrolytes, Int. J. Electrochem. Sci., 3 (**2008**) 5, 597–608,

[26] P. Jeevanandam, S. Vasudevan, Arrhenius and non-Arrhenius conductivities in intercalated polymer electrolytes, J. Chem. Phys., 109 (**1998**) 18, 8109–8117, doi:10.1063/1.477459

[27] M. Shahbazi, A. Bahari, S. Ghasemi, Structural and frequency-dependent dielectric properties of PVP-SiO2-TMSPM hybrid thin films, Org. Electron., 32 (**2016**), 100–108, doi:10.1016/j.orgel.2016.02.012

[28] D. M. Alshangiti, M. M. Ghobashy, M. Madani, Preparation and Dielectric Property of TiO_2 Doping with Silver Dispersed in Polyvinyl Alcohol and Polyurethane (TiO_2@Ag/PVA-PU) Nanocomposite Materials, Asian J. Sci. Res., 13 (**2020**) 4, 244–252, doi:10.3923/ajsr.2020.244.252

[29] C. Baker, A. Pradhan, L. Pakstis, D. J. Pochan, S. I. Shah, Synthesis and antibacterial properties of silver nanoparticles, J. Nanosci. Nanotechnol., 5 (**2005**) 2, 244–249, doi:10.1166/jnn.2005.034